Conductance and Permeation of Monovalent Cations through Depletion-Activated Ca^{2+} Channels (I_{CRAC}) in Jurkat T Cells

Albrecht Lepple-Wienhues and Michael D. Cahalan
Department of Physiology and Biophysics, University of California at Irvine, California 92717 USA

ABSTRACT We studied monovalent permeability of Ca^{2+} release-activated Ca^{2+} channels (I_{CRAC}) in Jurkat T lymphocytes following depletion of calcium stores. When external free Ca^{2+} ($[Ca^{2+}]_o$) was reduced to micromolar levels in the absence of Mg^{2+}, the inward current transiently decreased and then increased approximately sixfold, accompanied by visibly enhanced current noise. The monovalent currents showed a characteristically slow deactivation (τ = 3.8 and 21.6 s). The extent of Na^+ current deactivation correlated with the instantaneous Ca^{2+} current upon readdition of $[Ca^{2+}]_o$. No conductance increase was seen when $[Ca^{2+}]_o$ was reduced before activation of I_{CRAC}. With Na^+ outside and Cs^+ inside, the current rectified inwardly without apparent reversal below 40 mV. The sequence of conductance determined from the inward current at −80 mV was $Na^+ > Li^+ = K^+ > Rb^+ \gg Cs^+$. Unitary inward conductance of the Na^+ current was 2.6 pS, estimated from the ratios $\Delta\sigma^2/\Delta I$mean at different voltages. External Ca^{2+} blocked the Na^+ current reversibly with an IC_{50} value of 4 μM. Na^+ currents were also blocked by 3 mM Mg^{2+} or 10 μM La^{3+}. We conclude that I_{CRAC} channels become permeable to monovalent cations at low levels of external divalent ions. In contrast to voltage-activated Ca^{2+} channels, the monovalent conductance is highly selective for Na^+ over Cs^+. Na^+ currents through I_{CRAC} channels provide a means to study channel characteristics in an amplified current model.

INTRODUCTION

A highly selective Ca^{2+} current in lymphoid and mast cells has been characterized and named I_{CRAC} to signify its activation by calcium release from intracellular stores (Lewis and Cahalan, 1989; Hoth and Penner, 1992; Zweifach and Lewis, 1993). Similar currents have also been described in a wide variety of nonexcitable cells, including rat basophilic leukemia (RBL) cells, macrophages, fibroblasts, thyrocytes, hepatocytes, a colonic epithelial cell line, *Xenopus* oocytes (for reviews see Fasolato et al., 1994; Lewis and Cahalan, 1995), and melanoma cell lines (Lepple-Wienhues and Cahalan, 1995). Different depletion-activated currents have been reported in vascular endothelium and epidermal cancer cells (Vaca and Kunze, 1994; Lückhoff and Clapham, 1994). They resemble the insect trp gene product in their poor selectivity for divalent over monovalent cations and single channel conductances in the 10 pS range. I_{CRAC} channels may represent a family of related Ca^{2+} entry channels that are involved in calcium homeostasis and signaling in diverse cell types. In T cells, I_{CRAC} provides the major Ca^{2+} influx pathway controlling basic cellular functions such as interleukin-2 gene expression, secretion, and cell proliferation (Zweifach and Lewis, 1993; Negulescu et al., 1994). I_{CRAC} currents are not voltage-operated, but open following depletion of intracellular Ca^{2+} stores. I_{CRAC} can be distinguished from other store-operated currents by its high selectivity for Ca^{2+} and a unitary conductance well below 1 pS. In the absence of extracellular Ca^{2+} monovalent currents have been observed (Hoth and Penner, 1993; McDonald et al., 1993; Premack et al., 1994). Organic blockers of voltage-operated Ca^{2+} channels do not inhibit I_{CRAC} (Premack et al., 1994). Albeit nonspecific, the trivalent metals La^{3+} and Gd^{3+} are the most potent inhibitors (Hoth and Penner, 1993; Ross and Cahalan, 1995) Anomalous mole-fraction behavior for Ba^{2+} and Ca^{2+} has been described (Hoth, 1995). The mechanisms linking store- depletion and membrane current are still unknown. Involvement of small G proteins, a soluble messenger, and vesicular fusion have been suggested as activation pathways (Fasolato et al., 1993; Parekh et al., 1993; Randriamampita and Tsien, 1993; Somasundaram et al., 1995). Inactivation of the current has been shown to depend on intracellular Ca^{2+}, the type of chelator used in the pipette, and protein kinases (Hoth and Penner, 1993; Zweifach and Lewis, 1995a; Zweifach and Lewis, 1995b; Parekh and Penner, 1995). Noise analysis of Ca^{2+} currents has provided evidence for discretely gating channels in T cells with an estimated conductance of 24 fS in high external Ca^{2+}. This unitary conductance does not allow examination of single channel currents using available techniques. A conductance of 24 fs is extremely small for an ion channel, giving an estimate of >10,000 channels per cell (Zweifach and Lewis, 1993).

In the present study we examined the permeation properties of I_{CRAC} channels for monovalent cations and the divalent block of monovalent currents. Macroscopic channel noise with Na^+ as the charge carrier was analyzed to gain further insight into channel properties. A preliminary report has appeared (Lepple-Wienhues and Cahalan, 1996).

Received for publication 8 March 1996 and in final form 1 May 1996.

Address reprint requests to Dr. Michael D. Cahalan, Department of Physiology and Biophysics, University of California at Irvine, Irvine, CA 92717, Tel.: 714-824-7260; Fax: 714-824-8540; E-mail: mcahalan@uci.edu.

0006-3495/96/08/787/08 $2.00

MATERIALS AND METHODS

Cell culture

The human leukemia T-cell line Jurkat E6–1 was obtained from the American Type Culture Collection (Rockville, MD) and maintained in RPMI 1640/10% fetal calf serum media. The cells were passed twice weekly and kept at a low density (< 10^5/ml). For patch clamp experiments cells were allowed to settle on poly-D-lysine-coated coverslips.

Solutions

Intracellular solutions contained (mM): 128 Cs aspartate, 10 Cs-*N*-[2-hydroxyethyl]piperazine-*N'*-[2-ethanesulfonic acid (HEPES, pH 7.2), and either 12 1,2-bis(2-aminophenoxy)ethane-*N,N,N',N'*-tetraacetic acid (BAPTA), 0.9 $CaCl_2$, 3.16 $MgCl_2$ or 12 ethyleneglycol-bis(β-Aminoethylether)*N,N,N',N'*-tetraacetic acid (EGTA), 0.7 $CaCl_2$, 3.0 $MgCl_2$. Free $[Ca^{2+}]$ was 10 nM as measured using fura-2 ratios. 10 μM inositol 1,4,5-trisphosphate (IP_3) was added when indicated. The composition of external solutions is summarized in Table 1. External solutions used for permeability studies were prepared by titrating methanesulfonic acid using the hydroxide of the respective cation. EGTA stock solutions saturated with Ca^{2+} and Mg^{2+} were prepared using a pH-metric method (Neher, 1988). Free $[Ca^{2+}]_o$ and $[Mg^{2+}]_o$ levels were calculated using "Chelator" software (Theo J.M. Schoenmakers, University of Nijmegen, The Netherlands). NaOH and KOH were purchased from Fischer Scientific (Fair Lawn, NJ); LiOH and RbOH from Johnson Matthey Electronics (Ward Hill, MA); CsOH from Fluka Chemie (Buchs, Switzerland); charybdotoxin from Peptide Institute (Osaka, Japan); and HEPES from Calbiochem (La Jolla, CA). All other chemicals were purchased from Sigma (St. Louis, MO).

Patch clamp recording

Whole-cell currents were recorded using an EPC-9 patch clamp amplifier (HEKA, Lambrecht, Germany). Patch pipettes were pulled from soft glass capillaries (Accu-fill 90 Micropets, Becton, Dickinson and Co., Parsippany, NJ), sylgard coated (Dow Corning Corp., Midland, MI), and fire-polished to 2–4 MΩ resistance in Ringer. Amplifier control and data recording were performed using a Macintosh Quadra 700 microcomputer (Apple Computer, Cupertino, CA). Data were sampled at 5–10 kHz and digitally filtered at 0.5 kHz for analysis and display. Fast and slow capacitive transients were canceled using the compensation circuitry of the EPC-9. Series resistance (5–10 MΩ) was not compensated. Voltage was corrected for liquid junction potentials. Fast solution exchange was achieved using a mobile linear array of wide-tipped puffer pipettes. The solution exchange time estimated from the block of Na^+ current by Ca^{2+} and the removal of block when Ca^{2+} was washed out was <150 ms. The reference electrode was connected using a Ringer agar bridge. All experiments were performed at room temperature (22–25°C). For noise analysis, data were sampled at 5 kHz and digitally low-pass-filtered at 1 kHz. To eliminate low frequency components (<10 Hz) from power spectra, a third-order polynomial fit was performed on continuous traces and subtracted. To obtain current variance, 500-ms intervals of traces were digitally low-pass-filtered at 700 Hz. During this sampling interval, the mean current changed by <10%. Analysis was performed using the programs Pulse (HEKA, Lambrecht, Germany) and Igor Pro (Wavemetrics, Lake Oswego, Oregon).

RESULTS

The depletion-activated channel is permeable to Na^+ when external divalent cations are removed

Following activation of I_{CRAC} by depletion of intracellular Ca^{2+} stores, withdrawal of external divalent ions revealed a monovalent conductance much larger than that carried by Ca^{2+} ions. This conductance was observed only when the concentration of external divalent cations was reduced to micromolar levels or lower. Fig. 1 shows a typical experiment. Intracellular Ca^{2+} stores were depleted using 10 μM IP_3 and 12 mM BAPTA in the pipette. $[Ca^{2+}]_o$ was varied as indicated, and Na^+ was the only monovalent cation present in the low $[Ca^{2+}]_o$ solution, which contained no Mg^{2+}. I_{CRAC} developed within 20 s of break-in as IP_3 reduced the Ca^{2+} content of the stores. When $[Ca^{2+}]_o$ was

TABLE 1 External solutions

Solution	$[Na^+]$	$[K^+]$	$[X^+]$	$[Ca^{2+}]$ (total)	pCa (free)	$[Mg^{2+}]$ (total/free)	$[Cl^-]$	$[CH_3SO_3^-]$	[Chelator]
1	120	5	—	20	1.7	—/—	165	—	—
2	160	5	—	2	2.7	—/—	169	—	—
3	160	5	—	0.1	4	—/—	165	—	—
4	160	5	—	1.8	5	—/—	165	—	2 HEDTA
5	160	5	—	1.8	6	—/—	165	—	2 EGTA
6	160	5	—	0.88	7	—/—	165	—	2 EGTA
7	160	5	—	0.15	8	—/—	165	—	2 EGTA
8	160	5	—	1.2	5	3.7/3	165	—	2 HEDTA
9	160	5	—	0.25	6	4.4/3	165	—	2 HEDTA
10	—	—	120 NMG^+	20	1.7	—/—	2	158	—
11	120	—	—	20	1.7	—/—	2	158	—
12	160	—	—	1.8	6	—/—	2	158	2 EGTA
13	—	—	160 Rb^+	1.8	6	—/—	2	158	2 EGTA
14	—	—	160 Cs^+	1.8	6	—/—	2	158	2 EGTA
15	—	—	160 K^+	1.8	6	—/—	2	158	2 EGTA
16	—	—	160 Li^+	1.8	6	—/—	2	158	2 EGTA
17	—	—	160 NMG^+	1.8	6	—/—	2	158	2 EGTA
18	—	—	160 NMG^+	—	~5	—/—	2	158	—

Concentrations in mM. All solutions contained 10 mM HEPES and 5 mM glucose, and were titrated to pH 7.4 ($CH_3SO_3^-$ = methanesulphonate, NMG^+ = N-methyl-D-glucamine, HEDTA = N-hydroxyethyl-ethylenediamine-triacetic acid). 0.1 μM charybdotoxin was present in K^+- and Rb^+-containing solutions to block current through K^+ channels.

reduced to 1 and 10 μM, a larger inward Na^+ current was revealed that inactivated. In five similar experiments, the ratio of Na^+ to Ca^{2+} current averaged 6.4 ± 1.3 (pCa = 6 vs. pCa = 1.7), with a maximal Na^+ conductance of 448 ± 67 pS (n = 5). Readdition of 20 mM $[Ca^{2+}]_o$ enabled the smaller Ca^{2+} current to redevelop. The I-V relations of both Na^+ and Ca^{2+} currents were strongly inward rectifying (Fig. 1 *B*) and no measurable outward current developed during inactivation. These results suggest that I_{CRAC} channels become permeable to Na^+ when Ca^{2+} is reduced to the micromolar range, a property shared with voltage-gated Ca^{2+} channels (Hess and Tsien, 1984; Almers et al., 1984).

Inactivation of Na^+ currents correlates with subsequent reactivation of Ca^{2+} currents

When IP_3 was omitted from the pipette solution, passive store depletion was slow allowing several solution changes before induction of the current. As shown in Fig. 2*A*, Na^+ current could not be evoked when $[Ca^{2+}]_o$ was removed before activation of the Ca^{2+} current. Ca^{2+} and Na^+ currents were induced in parallel by slow passive store depletion with a strong correlation between the magnitudes of Ca^{2+} currents and peak Na^+ currents (Fig. 2*A*, *inset*).

Na^+ currents activated by stores depletion showed a characteristically slow inactivation (Figs. 1 *A* and 2 *A*, see also Hoth and Penner, 1993), resembling the kinetics of slow Ca^{2+} dependent activation of depletion-activated Ca^{2+} currents (Zweifach and Lewis, 1996). Slow inactivation of Na^+ currents in the virtual absence of Ca^{2+} may therefore represent a reversal of the slow activation of Ca^{2+} currents, which is known to depend on the extracellular Ca^{2+} concentration. To test this hypothesis, we varied the duration of $[Ca^{2+}]_o$ reduction, allowing for different degrees of Na^+ current inactivation. When external Ca^{2+} was raised before the Na^+ currents were completely inactivated, the subsequent instantaneous Ca^{2+} current (upon readmission of Ca^{2+}) was larger. When Na^+ currents in low $[Ca^{2+}]_o$ inactivated completely, the instantaneous Ca^{2+} current was reduced. Fig. 2 *B* shows a clear correlation between the instantaneous Ca^{2+} current and the extent of Na^+ current inactivation. Both the inactivation of Na^+ currents and the subsequent activation of Ca^{2+} currents could be well fitted using double exponentials. These parallels in the development and inactivation of Na^+ and Ca^{2+} current provide strong evidence that both currents are carried through I_{CRAC} channels.

Ca^{2+} currents through I_{CRAC} channels undergo rapid inactivation within several tens of ms, probably because of binding of Ca^{2+} to sites close to the inner channel mouth (Zweifach and Lewis, 1995a). This inactivation depends on the type of the intracellular chelator and is also seen in RBL cells (Hoth and Penner, 1993). As shown in Fig. 2 *C*, the Na^+ current does not undergo rapid inactivation as seen with the Ca^{2+} current, providing further evidence that this rapid inactivation depends on Ca^{2+} entry.

Monovalent selectivity sequence

Current-voltage relationships illustrated in Fig. 3 provide further evidence for Na^+ as the charge carrier with micromolar concentration of external divalent cations. The positive reversal potential indicates a poor permeability to Cs^+ (Figs. 1 *B* and 3 *A*). In most cells when external Na^+ was replaced by Cs^+, the conductances for NMG^+ and Cs^+ were indistinguishably low within the studied voltage range. However, some cells displayed an additional nonspecific cation conductance with similar permeability for Cs^+ and Na^+. This "leak" conductance showed linear I-V relations and lacked the characteristically slow inactivation. Neglecting cells with a large leak component, we alternated $[Ca^{2+}]_o$ between 20 mM and 1 μM to determine the inactivating component of monovalent whole cell currents. Fig. 3 *B* shows membrane currents in solutions containing Na^+, Li^+, K^+, and NMG^+ as the only cations at 1 μM $[Ca^{2+}]_o$. Evidently, the channels are highly selective for Na^+ over Cs^+ even in the virtual absence of divalent cations. The sequence of conductance estimated from inward current

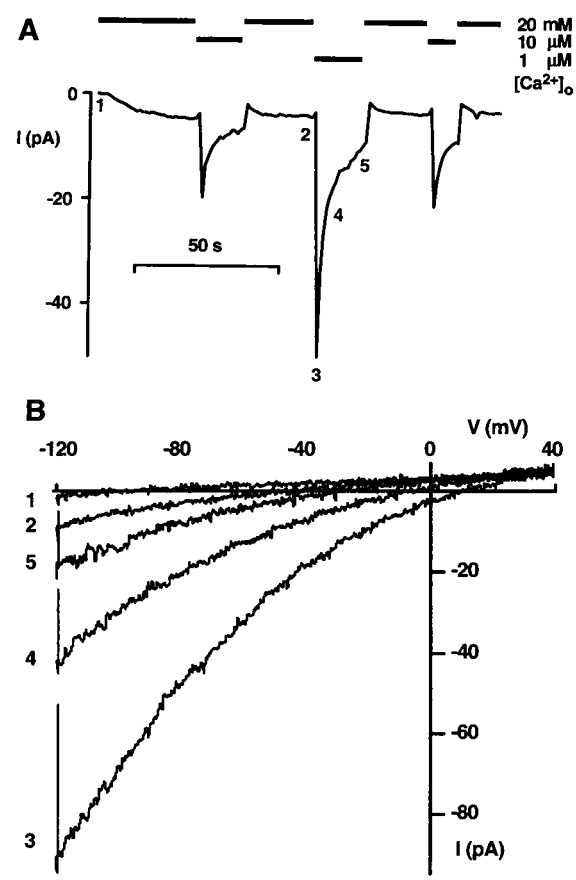

FIGURE 1 Inward current induced by IP_3-mediated store depletion at 1 μM, 10 μM and 20 mM $[Ca^{2+}]_o$. (*A*) Following activation of I_{CRAC} in 20 mM $[Ca^{2+}]_o$, a Na^+ current is unmasked by lowering $[Ca^{2+}]_o$ to 1 or 10 μM. Inward currents at −80 mV were obtained using 200-ms voltage ramps repeated at 1 s intervals (holding potential −20 mV). (*B*) Ramp currents at the indicated times were filtered at 700 Hz and not leak subtracted. The pipette contained 12 mM BAPTA (Solutions 1, 4 and 5).

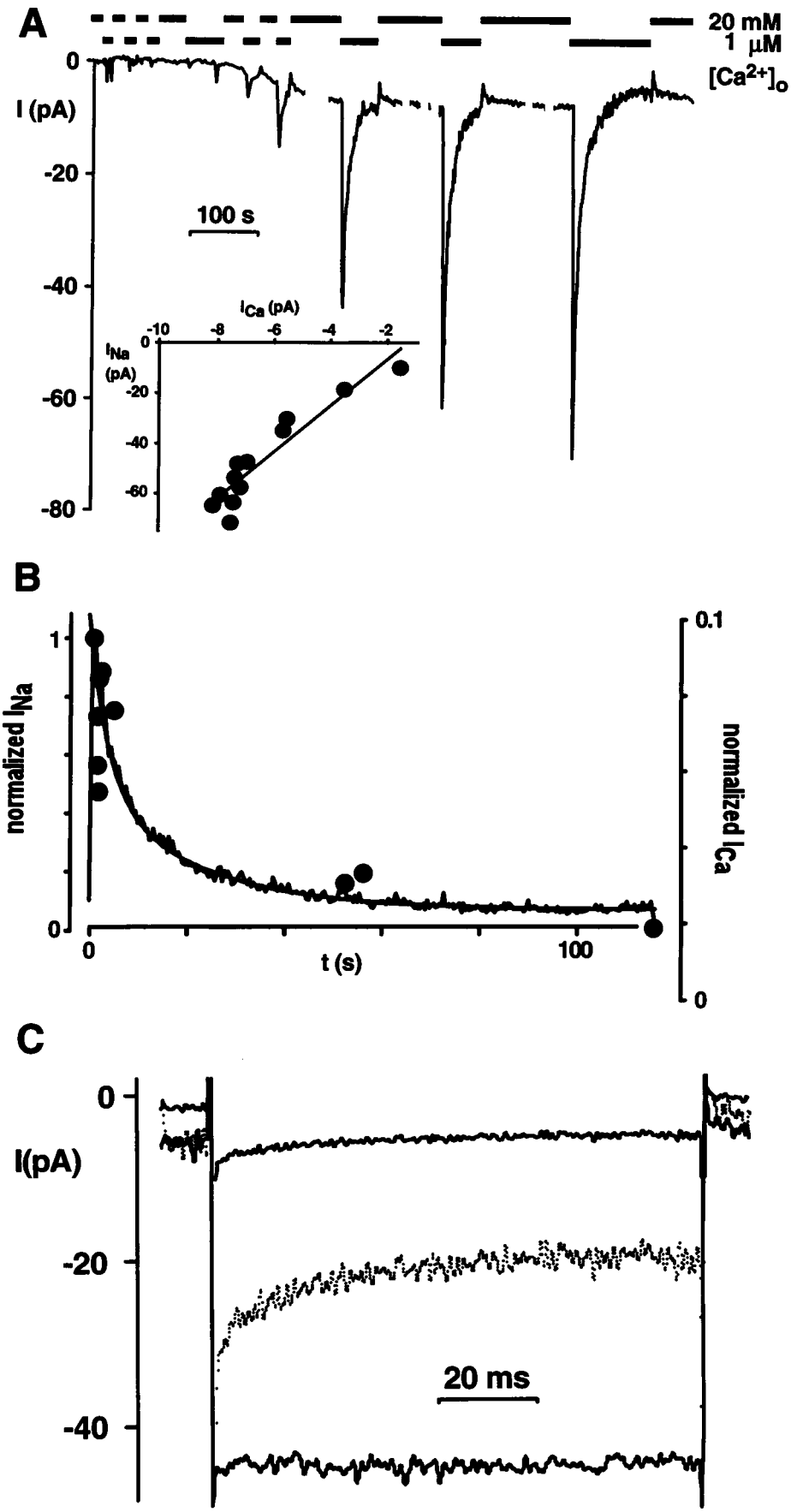

FIGURE 2 Development and inactivation of Na^+ and Ca^{2+} current through I_{CRAC} channels. (*A*) Parallel induction of Na^+ and Ca^{2+} currents following slow passive store depletion (12 mM BAPTA, no IP_3). (*inset*) Ca^{2+} current plateaus are plotted against subsequent peak Na^+ currents, showing the simultaneous induction of both currents. Note the lack of Na^+ current when $[Ca^{2+}]_o$ is lowered before store depletion. Spontaneous small inward current spikes were seen in some cells (cf. Zweifach and Lewis, 1993). Short pulses of 1 μM $[Ca^{2+}]_o$ could not be resolved at this time scale and were left out for clarity. Currents were obtained using pulses of 100 ms duration from −20 to −100 mV every 400 ms. Six pulses obtained immediately after disruption of the membrane were averaged and subtracted. (*B*) Inactivation of Na^+ currents determines instantaneous Ca^{2+} currents. When $[Ca^{2+}]_o$ was raised back to 20 mM following variable intervals of 1 μM $[Ca^{2+}]_o$, the subsequent instantaneous Ca^{2+} current (●) closely followed the extent of Na^+ current inactivation. Approximately 20% of the instantaneous Ca^{2+} current remained following prolonged Na^+ current inactivation. Current data were fitted using double exponential functions with time constants and amplitude coefficients (in parentheses) normalized to peak Na^+ current: τ = 3.8 s (0.58) and 21.6 s (0.42) for the inactivation of the Na^+ current and τ = 1.2 s (0.11) and 14.8 s (0.05) for the activation of the Ca^{2+} current (not shown). Ca^{2+} currents are shown at a magnified scale with an offset of 0.02. (*C*) Rapid inactivation is seen with Ca^{2+} (*upper trace*), but not Na^+ (*lower trace*) as the charge carrier. 100-ms pulses from −20 to −120 mV were applied. Four subsequent pulses were averaged and leak-subtracted using pulses before activation of the current. The dashed trace shows the Ca^{2+} current magnified four times (solutions 10 and 12).

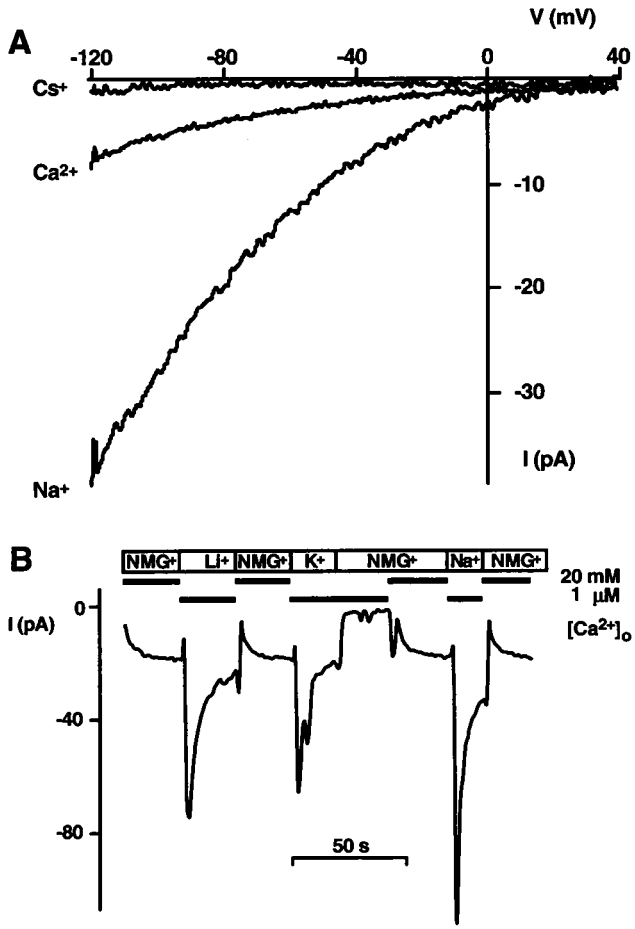

FIGURE 3 Monovalent current through I_{CRAC} channels. (*A*) Whole cell currents in response to voltage ramps (−120 to 40 mV for a duration of 200 ms, holding potential −20 mV). Currents in 20 mM Ca^{2+} (with 120 mM NMG^+) and 160 mM Na^+ (10^{-6} M Ca^{2+}) outside were inwardly rectifying and did not reverse up to 40 mV. 160 mM Cs^+ (10^{-6} M Ca^{2+}) carried only a minuscule inward current. Leak current was determined with 160 mM NMG^+ (10^{-6} M Ca^{2+}) and subtracted (solutions 10, 12, and 17). (*B*) Conductance for Na^+, Li^+, K^+, and NMG^+ seen as inward currents at −80 mV. The slowly activating current with the NMG^+ solution containing 20 mM Ca^{2+} was carried by Ca^{2+}. The short transient before activation of the Ca^{2+} current in NMG^+ solution is an artifact. Ramps obtained before current activation were subtracted (solutions 10, 12, and 15–17).

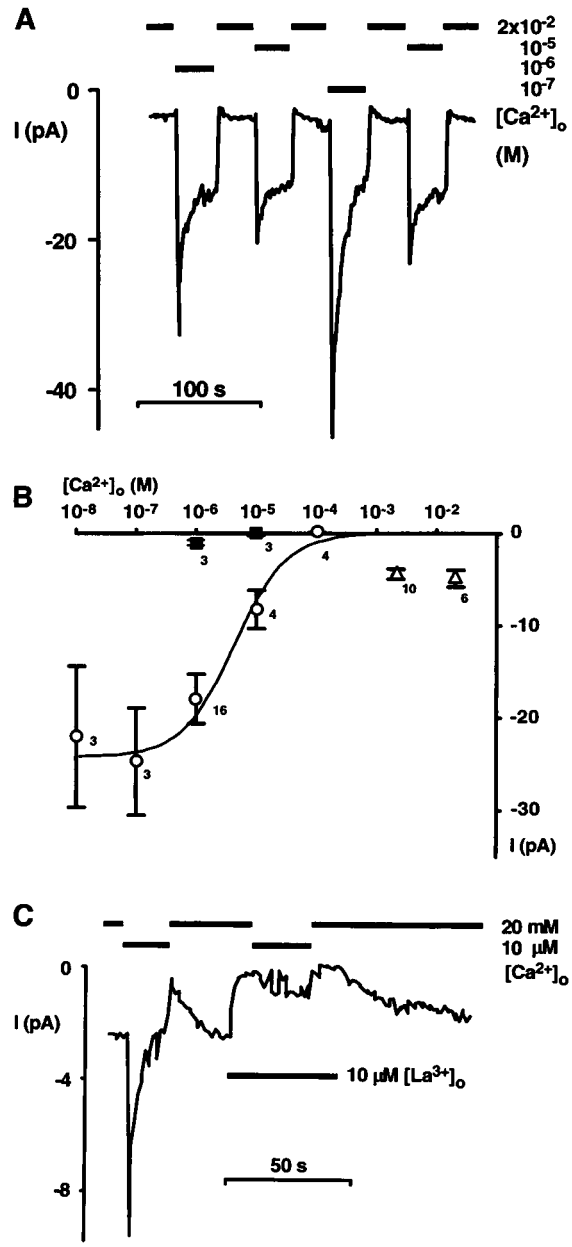

FIGURE 4 Block of Na current through I_{CRAC} channels by Ca^{2+} and La^{3+}. (*A*) Inactivating Na^+ currents at different $[Ca^{2+}]_o$ levels. Currents were activated using 10 μM IP_3 in the pipette (Solutions 1 and 4–6, ramp currents at −80 mV measured as in Fig. 1). (*B*) Inward current at −80 mV as a function of $[Ca^{2+}]_o$. The inactivating component of the Na^+ current (○) was obtained by subtracting the steady-state current from the peak current. The line represents a Michaelis-Menten fit assuming a Hill coefficient of 1. Mg^{2+} in the bath (3 mM) blocked the current at $[Ca^{2+}]_o \leq 10^{-5}$ M (■). Steady-state Ca^{2+} currents were plotted for comparison (Δ) (Solutions 1–9). (*C*) La^{3+} blocks Ca^{2+} currents and inactivating Na^+ currents reversibly. Na^+ is the main cation throughout the experiment. The low $[Ca^{2+}]_o$ solution contains no chelators to avoid interactions with La^{3+} (ramp currents at −80 mV, solutions 10 and 18).

magnitudes is: $P_{Na} > P_{Li} = P_K > P_{Rb} \gg P_{Cs} \geq P_{NMG}$. We were unable to determine reversal potentials due to 1) the small Cs^+ currents, 2) inward rectification of the current, and 3) the tendency of seals to become leaky when the voltage was raised >40 mV at micromolar calcium levels.

Block of Na^+ current

Na^+ currents were blocked by extracellular Ca^{2+} in a dose-dependent manner. Fig. 4 *A* shows a typical experiment with transient Na^+ currents at different $[Ca^{2+}]_o$ levels. Similar experiments with $[Ca^{2+}]_o$ varying from submicromolar to millimolar levels are summarized in Fig. 4 *B*. Inactivating Na^+ currents become smaller at higher $[Ca^{2+}]_o$ levels, following an apparent simple one to one stoichiometry with an IC_{50} of 4 μM (pCa = 5.4, Hill coefficient of 1). At pCa = 4 no measurable inactivating Na^+ current could be observed. If $[Ca^{2+}]_o$ was raised further, a slowly activating

Ca^{2+} current was seen without slow inactivation (see above). The Ca^{2+} current was not altered by changing extracellular Na^+ concentration (not shown, cf. Hoth and Penner, 1993). Na^+ currents at pCa $\geq$ 5 were completely blocked by 1 mM extracellular Mg^{2+}. 10 μM La^{3+} blocked the Ca^{2+} current as well as the inactivating Na^+ current reversibly (Fig. 4 *C*). Na^+ currents were not altered when 1 μM tetrodotoxin was added (not shown).

Noise analysis of Na^+ currents

Fig. 5 *A* shows a continuous current recording from a cell voltage clamped at −60 mV. When $[Ca^{2+}]_o$ was rapidly reduced from 20 mM to 1 μM, a transient decline of current was followed by the development of a large inward current. The increase of mean current was accompanied by fluctuations seen as macroscopic current noise (Fig. 5 *B*). We determined mean current and current variance at different holding voltages in a series of 500-ms intervals during the slow inactivation phase, as shown in Fig. 5 *C*. Assuming a low open probability, the single channel conductance of I_{CRAC} channels carrying Na^+ current, as estimated from the slope in Fig. 5 *C*, is 2.6 pS. Power spectra were obtained from traces as shown in Fig. 5, *A* and *B*. Fig. 5 *D* shows the spectra of the Na^+ current fitted by eye using a single Lorentzian

$$S(f) = S(0)/[1 + (f/f_c)^2]$$

where $S(f)$ is the spectral current density at a given frequency f and f_c is the corner frequency. The corner frequency was f_c = 150 Hz, and the total variance $S(0) \times \pi \times f_c/2$ = 21 pA^2.

DISCUSSION

I_{CRAC} channels are activated by depletion of intracellular Ca^{2+} stores and underlie the Ca^{2+} influx essential for sustained Ca^{2+} signaling, gene expression, and proliferation of T lymphocytes (Lewis and Cahalan, 1989; Zweifach and Lewis, 1993; Negulescu et al., 1994). In mast cells, these

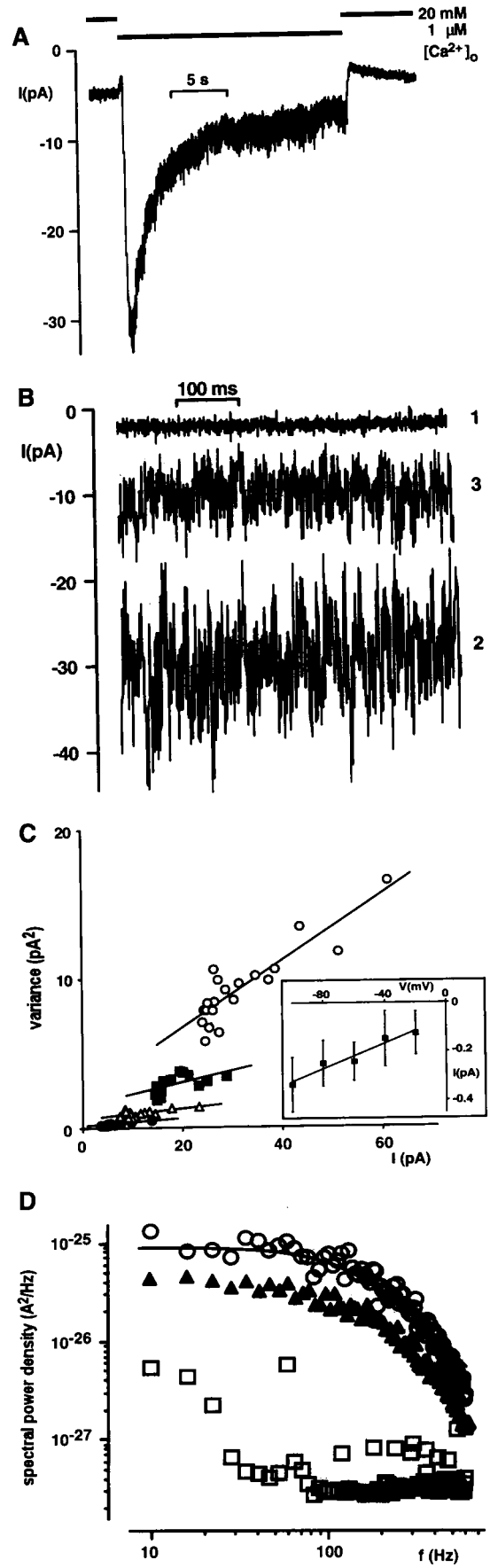

FIGURE 5 Noise analysis of Na^+ current through I_{CRAC} channels. (*A*) Continuous recording of inward current at −60 mV holding potential. $[Ca^{2+}]_o$ is altered between 20 mM and 1 μM as indicated (solutions 11 and 12). Note the slow activation/inactivation. (*B*) Current noise as seen during Na^+ current inactivation. 1 kHz filtering. Traces 1–3 show Ca^{2+} current, peak Na^+ current, and partially inactivated Na^+ current before, 1 s and 22 s after removal of $[Ca^{2+}]_o$, at −80 mV. (*C*) Variance versus mean current plotted at different holding potentials (○ −100, ■ −80, ▲ −60, and ● −20 mV, same cell as in A). Current traces were analyzed during inactivation of the Na^+ current (pCa = 6). The *inset* shows single-channel amplitudes estimated from slopes in the main panel (n = 4 cells). (*D*) Power spectral analysis of Na^+ currents. Power spectra were analyzed in a continuous current trace before (○) and after inactivation of the Na^+ current (▲) and with Ca^{2+} blocking the Na^+ current (□). The fit is a single Lorentzian described in the text (f_C = 150 Hz). Similar results were obtained in four cells.

channels mediate the immunoglobulin E response triggering secretion (Zhang and McCloskey, 1995).

Here we demonstrate that the I_{CRAC} channel, once activated, is permeable to Na^+ upon removal of extracellular Ca^{2+}. Several lines of evidence argue for the observed Na^+ current passing through the depletion-activated Ca^{2+} channel I_{CRAC}. 1) Ca^{2+} and Na^+ currents are the only measurable currents in store-depleted Jurkat cells when using Cs^+ as the main internal cation. T cells are electrically very tight, with only a limited number of ion channel types. The two prevailing K^+ channels and the swelling activated chloride channel do not contribute current using the described patch clamp protocol. Involvement of voltage activated Na^+ channels was ruled out using tetrodotoxin. 2) Na^+ and Ca^{2+} currents developed in parallel when stores were depleted slowly (Fig. 2 *A*). Na^+ currents as described here were never observed before store depletion took effect. 3) Slow inactivation of Na^+ currents reduced the subsequent magnitude of Ca^{2+} currents (Fig. 2 *B*). When Ca^{2+} was raised after a short period of Na^+ current, the instantaneous Ca^{2+} current was large. When, in contrast, the Na^+ current was allowed to inactivate fully, the subsequent Ca^{2+} current reactivated slowly starting with only a small instantaneous current. These data suggest that slow Ca^{2+}-dependent activation of Ca^{2+} currents is reversed at low external Ca^{2+} concentrations, seen as slow inactivation of Na^+ currents. 4) The trivalent rare earth La^{3+} is a potent blocker of both the Ca^{2+} and the Na^+ current. We therefore postulate, that the Na^+ current at low Ca^{2+} concentrations and the Ca^{2+} current in the presence of millimolar Ca^{2+} levels are conducted by the same channel.

The permeation of Na^+ provides strong evidence that the depletion-activated current is mediated by an ion channel, in agreement with previous reports (Hoth and Penner, 1992; Zweifach and Lewis, 1993; Hoth and Penner, 1993). The unitary Na^+ current estimated from variance and mean currents is rather large for an ion carrier, and both the macroscopically visible noise and the Lorentzian shape of the power spectrum are typical for a gated channel. A large shift in reversal potential was observed when extracellular Ca^{2+} was lowered using an intracellular potassium glutamate solution in mast cells (Hoth and Penner, 1993). This was probably due to an outward K^+ current through I_{CRAC} channels. Using Cs^+ as the main internal cation, no outward current developed and the reversal potential of Na^+ currents remained positive during inactivation (Fig. 1 *B*). We find that the unitary conductance of I_{CRAC} channels with Na^+ as the charge carrier is 2.6 pS when external Ca^{2+} is kept at 1 μM. This value is ~100 times the estimated single channel conductance for Ca^{2+} currents (Zweifach and Lewis, 1993), and therefore in a more common range for most ion channels. Whole cell Na^+ currents, however, are only ~6 times larger. The apparent discrepancy between increases in unitary and whole cell conductance could be explained by the observed Ca^{2+}-dependent activation of I_{CRAC} channels, assuming a current component that inactivates within the solution exchange time when reducing extracellular Ca^{2+}. This would produce an underestimate of the initial Na^+ current. However, even the faster component of the slow inactivation (τ = 3.8 s) would not account for a large error. A second possible explanation involves a likely change in channel kinetics induced by low $[Ca^{2+}]_o$. The open probability of the channels could be reduced under these conditions. In fact, spectral analysis reveals a faster channel gating. At 1 μM $[Ca^{2+}]_o$, the corner frequency of the Na^+ current spectrum is three times greater than the corner frequency of Ca^{2+} currents (45 Hz, Zweifach and Lewis, 1993). The number of open single channels obtained from whole cell Na^+ conductance and single channel conductance is 150–200 per cell. This number is roughly 50 times smaller than previous estimates from Ca^{2+} current measurements and may underestimate the total channel number due to a small open probability. On the other hand, analysis of the macroscopic Na^+ current noise is probably more accurate than the analysis of extremely small Ca^{2+} current fluctuations.

Ion permeation of I_{CRAC} channels and voltage-gated Ca^{2+} channels share the property of monovalent permeation in low divalent concentration. However, there are some striking differences in ion selectivity properties, both for monovalents and divalents. Divalent ion selectivity of I_{CRAC} channels is unusual when compared with other Ca^{2+} channels. The conductance sequence has been described as $Ca^{2+} > Ba^{2+} \approx Sr^{2+} \gg Mn^{2+}$ (Hoth and Penner, 1993). Newer findings have shown a higher Ba^{2+} permeability of I_{CRAC} channels in mast and RBL cells when compared with Jurkat cells, a strong voltage dependence of the I_{Ba}/I_{Ca} ratio and anomalous mole fraction behavior for Ca^{2+}/Ba^{2+} mixtures (Hoth, 1995). Our data suggest a high affinity site in the selectivity filter, which can be occupied by a single Ca^{2+} ion. This is in good agreement with findings in voltage-activated Ca^{2+} channels (Almers et al., 1984; Hess and Tsien, 1984), with the affinity for Ca^{2+} being slightly lower in I_{CRAC} channels (4 vs. ~1 μM). Recently, a single high-affinity Ca^{2+} binding site in the outer pore of voltage-gated Ca^{2+} channels has been demonstrated using site-directed mutagenesis (Ellinor et al., 1995). However, the complex and multiple actions of Ca^{2+} on I_{CRAC} channels demand caution when interpreting the apparent stoichiometry. As in voltage-activated Ca^{2+} channels, the existence of anomalous mole fraction behavior and the increase of Ca^{2+} current over the range of 0.1 to 10 mM strongly suggest the existence of additional Ca^{2+} binding sites with lower affinity within the pore. Mg^{2+} blocks monovalent currents; this is also seen in voltage-gated Ca^{2+} channels (Almers et al, 1984; Fukushima and Hagiwara, 1985). However, we find an unusual monovalent selectivity sequence at low $[Ca^{2+}]_o$, notable for a very low permeability to Cs^+ from either side of the membrane. Typical voltage-activated Ca^{2+} channels lose their ionic selectivity when extracellular Ca^{2+} is lowered, becoming permeable to monovalent ions including Na^+, Li^+, K^+, Rb^+, and Cs^+ (McCleskey and Almers, 1985; Hess et al., 1986). Although the high selectivity for Ca^{2+} over monovalents at high $[Ca^{2+}]_o$ points to a multi-

ion selectivity filter similar to other Ca^{2+} channels, I_{CRAC} channels show a high ionic selectivity even at micromolar external Ca^{2+}, when the selectivity for divalent ions is lost. Both the reversal potential and the mean currents show a high selectivity for Na^+ over Cs^+ under these conditions. We propose that the I_{CRAC} channel pore is considerably smaller than the pore of a typical voltage-gated Ca^{2+} channel, acting as a molecular sieve in addition to the presumed high affinity Ca^{2+} binding site.

The study of Na^+ currents through I_{CRAC} channels provides an enhanced current model permitting the examination of single channel characteristics. Observing currents in the virtual absence of Ca^{2+} allows separation of complicated Ca^{2+} dependent activation- inactivation mechanisms, several of which have been described to be involved in the regulation of this physiologically important channel.

We thank Diana Cooper and Dr. Lu Forrest for assistance with cell culture. This work was supported by National Institutes of Health grants NS14609 and GM41514, and by a fellowship from the Deutsche Forschungsgemeinschaft (Le 792/2).

REFERENCES

Almers, W., E. W. McCleskey, and P. T. Palade. 1984. A non-selective cation conductance in frog muscle membrane blocked by micromolar external calcium ions. *J. Physiol.* 353:565–583.

Ellinor, P. T., J. Yang, W. A. Sather, J. F. Zhang, and R. W. Tsien. 1995. Ca^{2+} channel selectivity at a single locus for high-affinity Ca^{2+} interactions. *Neuron.* 15:1121–1132.

Fasolato, C., B. Innocenti, and T. Pozzan. 1994. Receptor activated Ca^{2+} influx: how many mechanisms for how many channels? *Trends Pharmacol. Sci.* 15:77–83.

Fasolato, C., M. Hoth, and R. Penner. 1993. A GTP-dependent step in the activation mechanism of capacitative calcium influx. *J. Biol. Chem.* 268:20737–20740.

Fukushima, Y., and S. Hagiwara. 1985. Currents carried by monovalent cations through calcium channels in mouse neoplastic B lymphocytes. *J. Physiol.* 358:255–284.

Hess, P., and R. W. Tsien. 1984. Mechanism of ion permeation through calcium channels. *Nature.* 309:453–456.

Hess, P., J. B. Lansman, and R. W. Tsien. 1986. Calcium channel selectivity for divalent and monovalent cations. Voltage and concentration dependence of single channel current in ventricular heart cells. *J. Gen. Physiol.* 88:293–319.

Hoth, M. 1995. Calcium and barium permeation through calcium release-activated calcium (CRAC) channels. *Pflügers Arch. Eur. J. Physiol.* 430:315–322.

Hoth, M., and R. Penner. 1992. Depletion of intracellular calcium stores activates a calcium current in mast cells. *Nature.* 355:353–356.

Hoth, M., and R. Penner. 1993. Calcium release-activated calcium current in rat mast cells. *J. Physiol.* 465:359–386.

Lepple-Wienhues, A., and M. D. Cahalan. 1995. Two different calcium-influx pathways in melanoma cells are cell cycle-dependent. *Biophys. J.* 68:A122.

Lepple-Wienhues, A., and M. D. Cahalan. 1996. Monovalent cation permeation through stores-dependent Ca^{2+} channels (Icrac) in Jurkat T lymphocytes. *Biophys. J.* 70:A152.

Lewis, R. S., and M. D. Cahalan. 1989. Mitogen-induced oscillations of cytosolic Ca^{2+} and transmembrane Ca^{2+} current in human leukemic T cells. *Cell Regul.* 1:99–112.

Lewis, R. S., and M. D. Cahalan. 1995. Ca^{2+} and K^+ channels in lymphocytes. *Annu. Rev. Immunol.* 13:623–653.

Lückhoff, A., and D. E. Clapham. 1994. Calcium channels activated by depletion of internal calcium stores in A431 cells. *Biophys. J.* 67: 177–182.

McCleskey, E. W., and W. Almers. 1985. The Ca channel in skeletal muscle is a large pore. *Proc. Natl. Acad. Sci. USA.* 82:7149–7153.

McDonald, T. V., B. A. Premack, and P. Gardner. 1993. Flash photolysis of caged inositol 1,4,5-trisphosphate activates plasma membrane calcium current in human T cells. *J. Biol. Chem.* 268:3889–3896.

Negulescu, P. A., N. Shastri, and M. D. Cahalan. 1994. Intracellular calcium dependence of gene expression in single T lymphocytes. *Proc. Natl. Acad. Sci. USA.* 91:2873–2877.

Neher, E. 1988. The influence of intracellular Ca^{2+} concentration on degranulation of dialyzed mast cells from rat peritoneum. *J. Physiol.* 395:193–214.

Parekh, A. B., H. Terlau, and W. Stühmer. 1993. Depletion of $InsP_3$ stores activates a Ca^{2+} and K^+ current by means of a phosphatase and a diffusible messenger. *Nature.* 364:814–818.

Parekh, A. B., and R. Penner. 1995. Depletion-activated calcium current is inhibited by protein kinase in RBL-2H3 cells. *Proc. Natl. Acad. Sci. USA.* 92:7907–7911.

Premack, B. A., T. V. McDonald, and P. Gardner. 1994. Activation of Ca^{2+} current in Jurkat T cells following the depletion of Ca^{2+} stores by microsomal Ca^{2+}-ATPase inhibitors. *J. Immunol.* 152:5226–5240.

Randriamampita, C., and R. Y. Tsien. 1993. Emptying of intracellular Ca^{2+} stores releases a novel small messenger that stimulates Ca^{2+} influx. *Nature.* 364:809–814.

Ross, P. E., and M. D. Cahalan. 1995. Ca^{2+} influx pathways mediated by swelling or stores depletion in mouse thymocytes. *J. Gen. Physiol.* 106:415–444.

Somasundaram, B., J. C. Norman, and M. P. Mahaut-Smith. 1995. Primaquine, an inhibitor of vesicular transport, blocks the calcium-release-activated current in rat megakaryocytes. *Biochem. J.* 309:725–729.

Vaca, L., and D. L. Kunze. 1994. Depletion of intracellular Ca^{2+} stores activates a Ca^{2+} selective channel in vascular endothelium. *Am. J. Physiol.* 267:C920–C925.

Zhang, L., and M. A. McCloskey. 1995. Immunoglobulin E receptor-activated calcium conductance in rat mast cells. *J. Physiol.* 483:59–66.

Zweifach, A., and R. S. Lewis. 1993. Mitogen-regulated Ca^{2+} current of T lymphocytes is activated by depletion of intracellular Ca^{2+} stores. *Proc. Natl. Acad. Sci. USA.* 90:6295–6299.

Zweifach, A., and R. S. Lewis. 1995a. Rapid inactivation of depletion-activated calcium current (I_{CRAC}) due to local calcium feedback. *J. Gen. Physiol.* 105:209–226.

Zweifach, A., and R. S. Lewis. 1995b. Slow calcium-dependent inactivation of depletion-activated calcium current. Store-dependent and -independent mechanisms. *J. Biol. Chem.* 270:14445–14451.

Zweifach, A., and R. S. Lewis. 1996. Calcium-dependent potentiation of store-operated calcium channels in T lymphocytes. *J. Gen. Physiol.* 107:597–610.